Supplementary Information (SI) for Dalton Transactions.

Investigation into the viability of N,N-disubstituted-N'-acylthiourea copper(II) precursors for thermal deposition without the use of solvents and the affect precursor geometry has on the deposited composites.

William Daly,[a,b] David J. Otway,[a] Ian M. Povey,[b] Martyn E. Pemble,[a,b]

[a]School of Chemistry, University College Cork, Cork, Ireland

[b]Tyndall National Institute, Cork, Ireland

Corresponding email: dave.otway@ucc.ie

Supporting Information

Contents

Biological toxicity screening

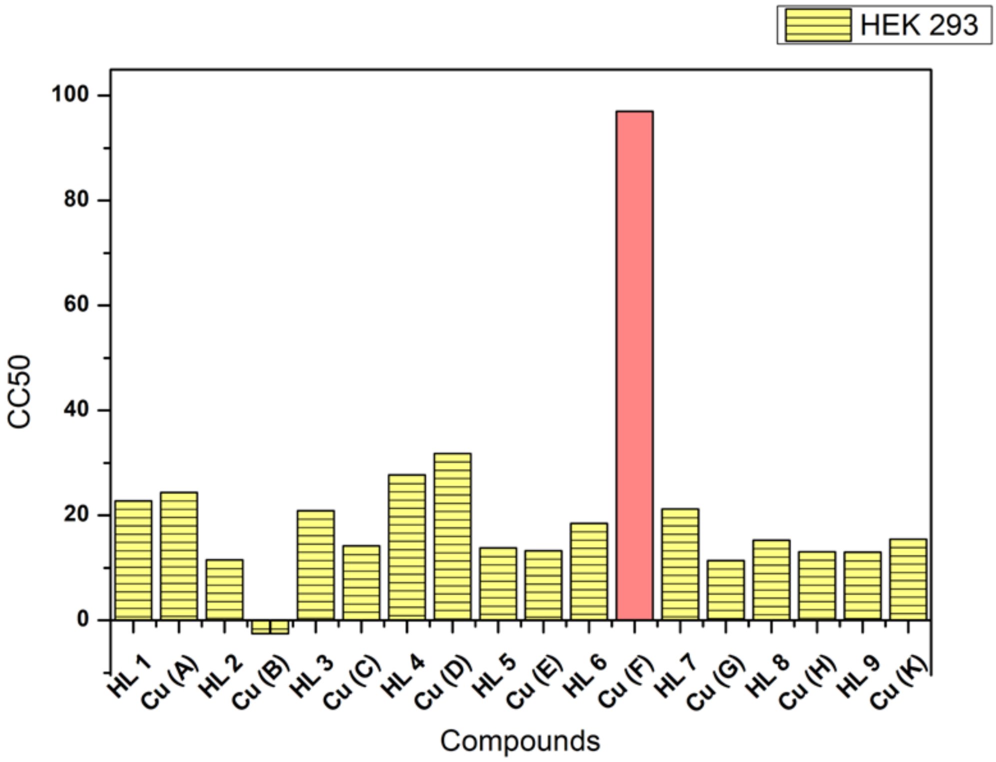

Figure 1 Cell viability (CC50) of ligands (HL) and copper(II) N,N-disubstituted-N'-acylthiourea complexes measured in HEK293 cells. All compounds exhibit low to moderate cytotoxicity 32 µg/mL (except for compound (F) which is flagged as highly toxic at <0.25 µg/mL.

Copper Sulfur single source precursors

Table 1 A brief snapshot of some copper-sulfur single source precursors

	Process Type	Precursor	TGA onset Temp (^0C)	Deposition Process Temp (^0C)	Deposition Substrate	Copper Sulfide	Comments	Ref
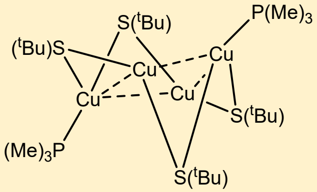	AASP	Thiolate $(CuS^tBu)_4(PMe_3)_2$	130	270	Glass	α-Cu_2S	Light sensitive Air sensitive	21
	AACVD-Toluene	Thiolate $(CuS^tBu)_4(PMe_3)_2$	130	270-300	Glass	α-Cu_2S	Light sensitive Air sensitive	34
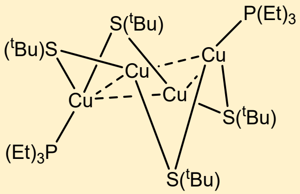	AACVD-Toluene	Thiolate $(CuS^tBu)_4(PEt_3)_2$	130	270-300	Glass	α-Cu_2S	Light sensitive Air sensitive	34

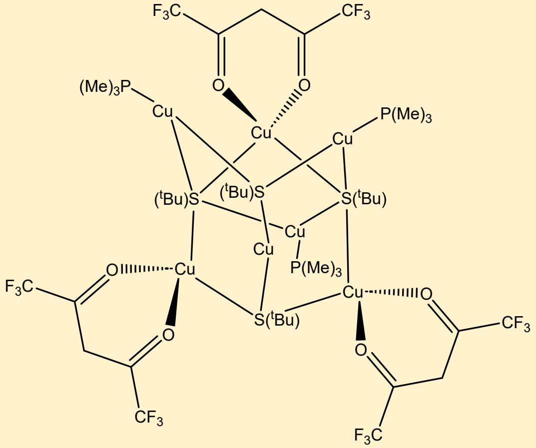	AACVD-Toluene	Thiolate $Cu_7(S^tBu)_4(hfa)_3(PMe_3)_3$	148	200-300	Glass	α-Cu_2S	Air sensitive	35
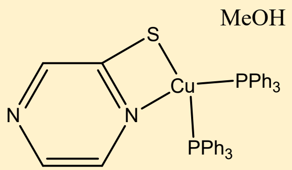	Solvent Assisted thermolysis	Thiolate $[Cu(spyz\text{-}2)(PPh_3)_2].MeOH$	240	200-800	---------	$Cu_{1.8}S$		36
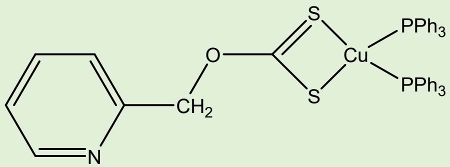	Thermolysis	Xanthate $(Cu(S_2O\text{-}pyCH_2O)(PPh_3)_2$ bis-(triphenylphosphine) *O*-methylpyridyl xanthate	130	100-800	---------	Cu_2S	Chugaev elimination	37
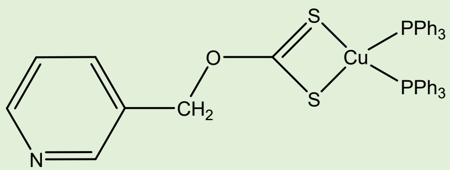	Thermolysis	Xanthate $(Cu(S_2M\text{-}pyCH_2O)(PPh_3)_2$ bis-(triphenylphosphine) *M*-methylpyridyl xanthate	160	100-800	---------	Cu_2S & CuS	Chugaev elimination	37
								37

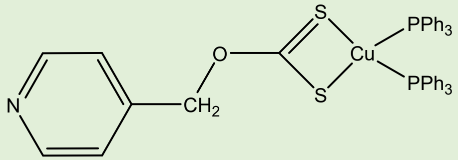	Thermolysis	Xanthate $(Cu(S_2\textit{P}\text{-}pyCH_2O)(PPh_3)_2$ bis-(triphenylphosphine) *P*-methylpyridyl xanthate	255	100-800	---------	Cu_2S & CuS	Chugaev elimination	
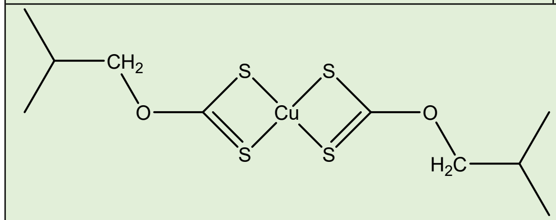	AACVD (Toluene)	Xanthtate $[Cu(SCSOCH_2CH(CH_3)_2)_2]$ Bis(*O*-isobutyldithiocarbonato)copper(II)	150	250 300 350	Glass	Covelite CuS	250-spherical 300-snowflake 350-flower	38
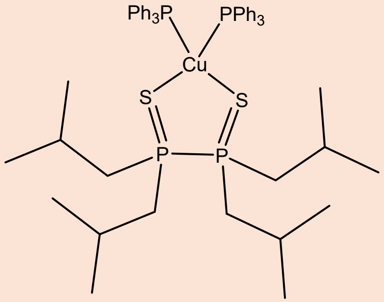	AACVD (Toluene)	Dialkyl $[Cu(^iBu_2PS_2)(PPh_3)_2]$	296	350-500	Glass	Cubic digenite $(Cu_{7.2}S_4)$ Rhombohedral digenite (Cu_9S_5)	Only at 400^0C pure mono phasic rhombohedral digenite Cu_9S_5	39
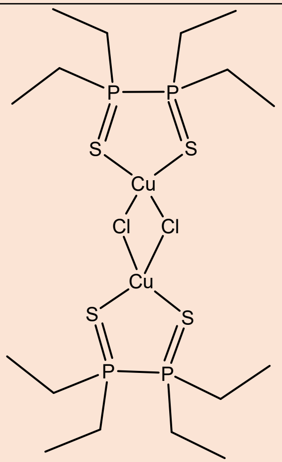	AACVD (CH_3CN)	$[Cu(S_2P_2Et_4)Cl]_2$ Tetraethyl diphosphine disulfide copper	134	400-450	Si	Cu_2S	Particles 60-100nm @ 400 Flakes 400nm @ 450	40
							350 – irregular	41

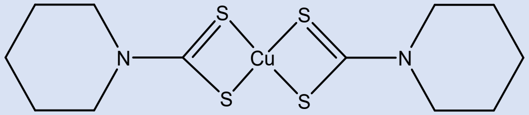	AACVD	Dithiocarbamates $Cu(S_2CN(piperidine))_2$ Bis(piperidinedithiocarbamato)copper(II)	220	350 400 450	Glass	Djurleite $Cu_{1.96}S$	morphology 400 - elongated morphology 450 – sphere & cubic mix	
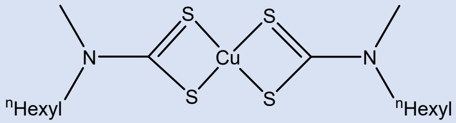	AACVD (Toluene)	Dithiocarbamates $Cu(S_2CNMe(^{n}Hexyl))_2$ Bis(N-methyl(^{n}Hexyl)dithiocarbamato)copper(II)	250	450	Glass	$Cu_{1.8}S$		[42]
	LP-MOCVD (Toluene)	Dithiocarbamates $Cu(S_2CNMe(^{n}Hexyl))_2$ Bis(N-methyl(^{n}Hexyl)dithiocarbamato)copper(II)	250	450	Glass	$Cu_{1.96}S$		[42]
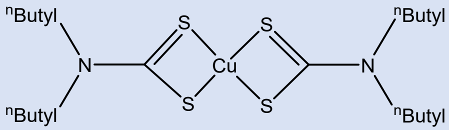	Thermolysis	Dithiocarbamates $Cu(S_2CN(^{n}Buty)_2)_2$ Bis(N-*di*-butyldithiocarbamato)copper(II)	233	250-300	Glass	Digenite $Cu_{2.9}S$		[43]
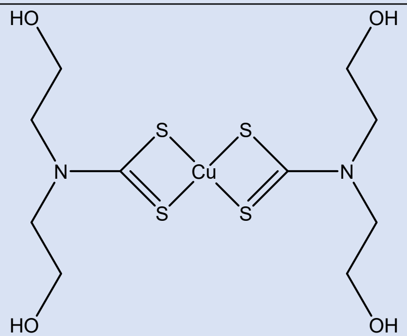	Thermolysis	Dithiocarbamates $Cu(S_2CNMe(CH_2CH_2OH))_2$ Bis(N-methyl(EtOH)dithiocarbamato)copper(II)	159	250-300	Glass	Digenite $Cu_{1.88}S$		[43]
		Dithiocarbamates			Si		Minor CuS incorporation	[44]

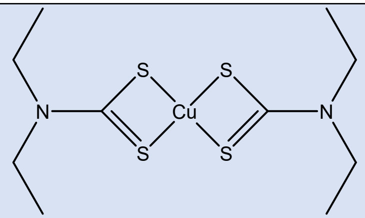	MOCVD	$Cu(S_2CN(Et_2)_2)_2$ Bis(diethyldithiocarbamato)copper(II)	200	300-500	Quarts Glass	$Cu_{1.96}S$	at shorter timed growth cycles	
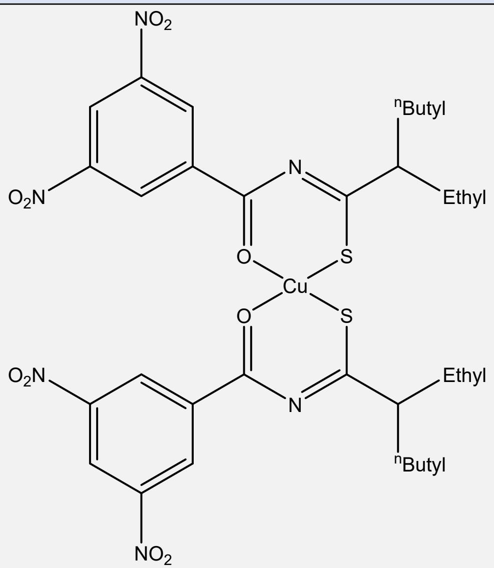	AACVD (THF)	Thiobiurets $[(Ethyl(^nButyl)NC(S)NC(O)C_6H_3(NO_2)\text{-}3,5]_2Cu(II)$ *N*-[ethyl(butyl)carbamothioyl]-3,5-dinitrobenzamide copper(II)	38	350	Glass	Monoclinic roxbyite (Cu_7S_4) Orthorhombic anilite (Cu_7S_4)	Scherrer relation grain size for all phases 49.5-65.8 nm	45

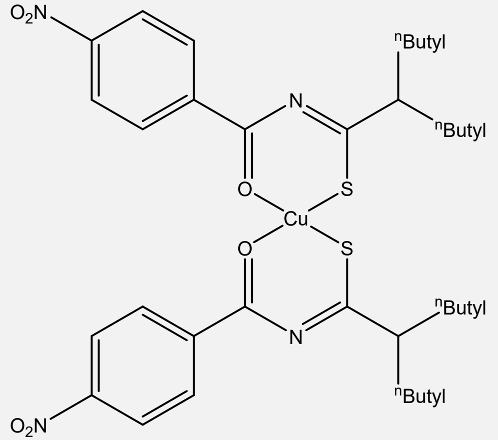	AACVD (Toluene)	Thiobiurets [(^{n}Butyl)$_2$)NC(S)NC(O)$C_6H_4(NO_2)$-3,5]$_2$Cu(II) *N*-[butyl(butyl)carbamothioyl]-4-nitrobenzamide copper(II)	180	350	Glass	Monoclinic roxbyite (Cu_7S_4)	49.5-65.8 nm	[46]
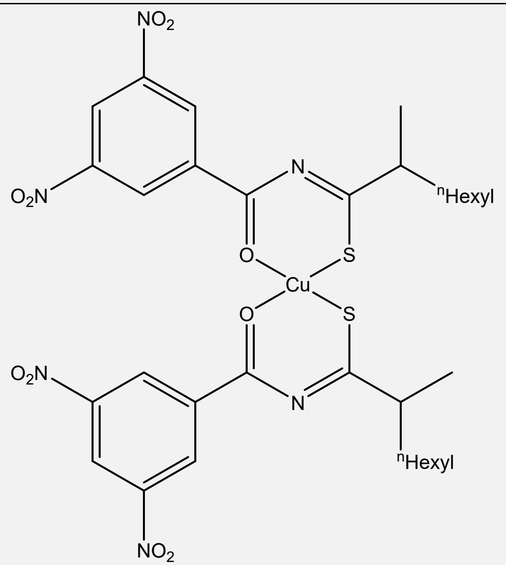	AACVD (Toluene)	Thiobiurets [(Methyl(^{n}Hexyl)NC(S)NC(O)$C_6H_3(NO_2)$-3,5]$_2$Cu(II) *N*-[metyl(hexyl)carbamothioyl]-3,5-dinitrobenzamide copper(II)	164	350	Glass	Orthorhombic anilite (Cu_7S_4)	49.5-65.8 nm	[46]

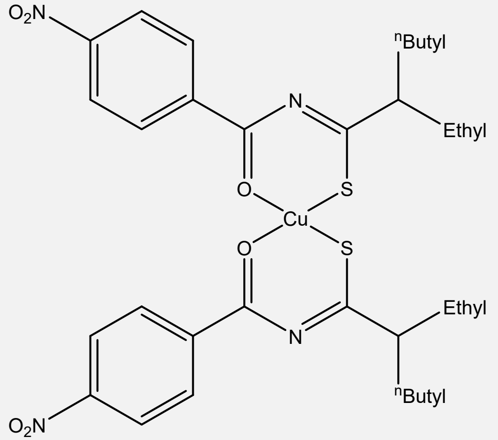	AACVD (Toluene)	Thiobiurets [(Ethyl(^{n}Butyl)NC(S)NC(O)$C_6H_3(NO_2)$-3,5]$_2$Cu(II) *N*-[ethyl(butyl)carbamothioyl]-3,5-dinitrobenzamide copper(II)	41	350	Glass	Rhombohedral digenite (Cu_9S_5)	49.5-65.8 nm	46
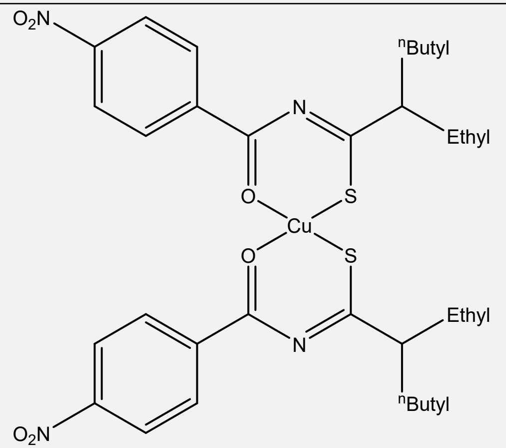	AACVD (Toluene)	Thiobiurets [(Ethyl(^{n}Butyl)NC(S)NC(O)$C_6H_4(NO_2)$-4]$_2$Cu(II) *N*-[ethyl(butyl)carbamothioyl]-4-nitrobenzamide copper(II)	167	350	Glass	Rhombohedral digenite (Cu_9S_5)	49.5-65.8 nm	46

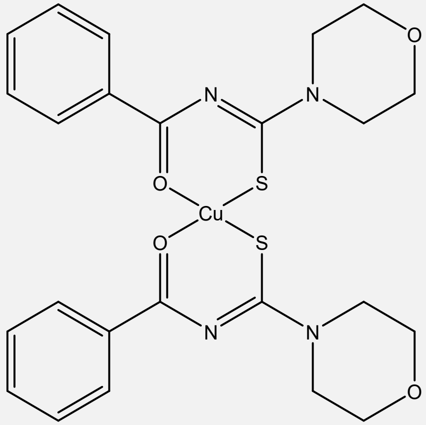	AACVD ($CHCl_3$)	Thiobiurets [(morpholine)NC(S)NC(O)C_6H_6]$_2$Cu(II) *N*-[(morpholine)carbamothioyl] copper(II)	180	350-450	Glass	Hexagonal (Cu_2S) Cubic (CuS_2)		47
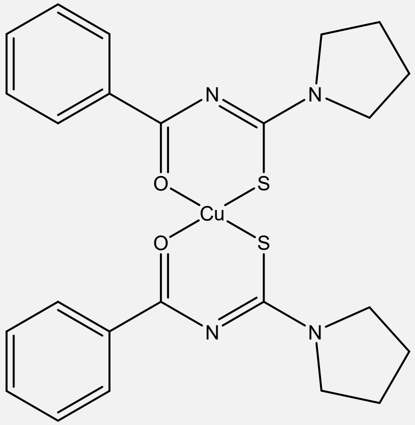	AACVD ($CHCl_3$)	Thiobiurets [(pyrrolidine)NC(S)NC(O)C_6H_6]$_2$Cu(II) *N*-[(pyrrolidine)carbamothioyl] copper(II)	205	350-450	Glass	Hexagonal (Cu_2S) Cubic (CuS_2)		47

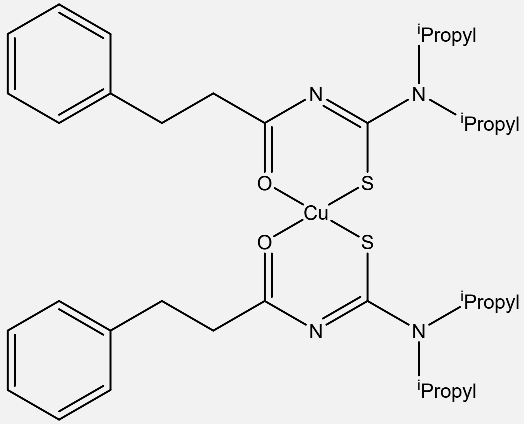	AACVD (THF)	Thiobiurets [(isoPropyl)$_2$NC(S)NC(O)CHCHPh]$_2$Cu(II) Bis(N,N-diisopropyl-N'-cinnamoylthiourea)copper(II)	145	350	Si/SiO$_2$	Unsuccessful		32

Stacked DSC analysis of the nine copper(II) complexes

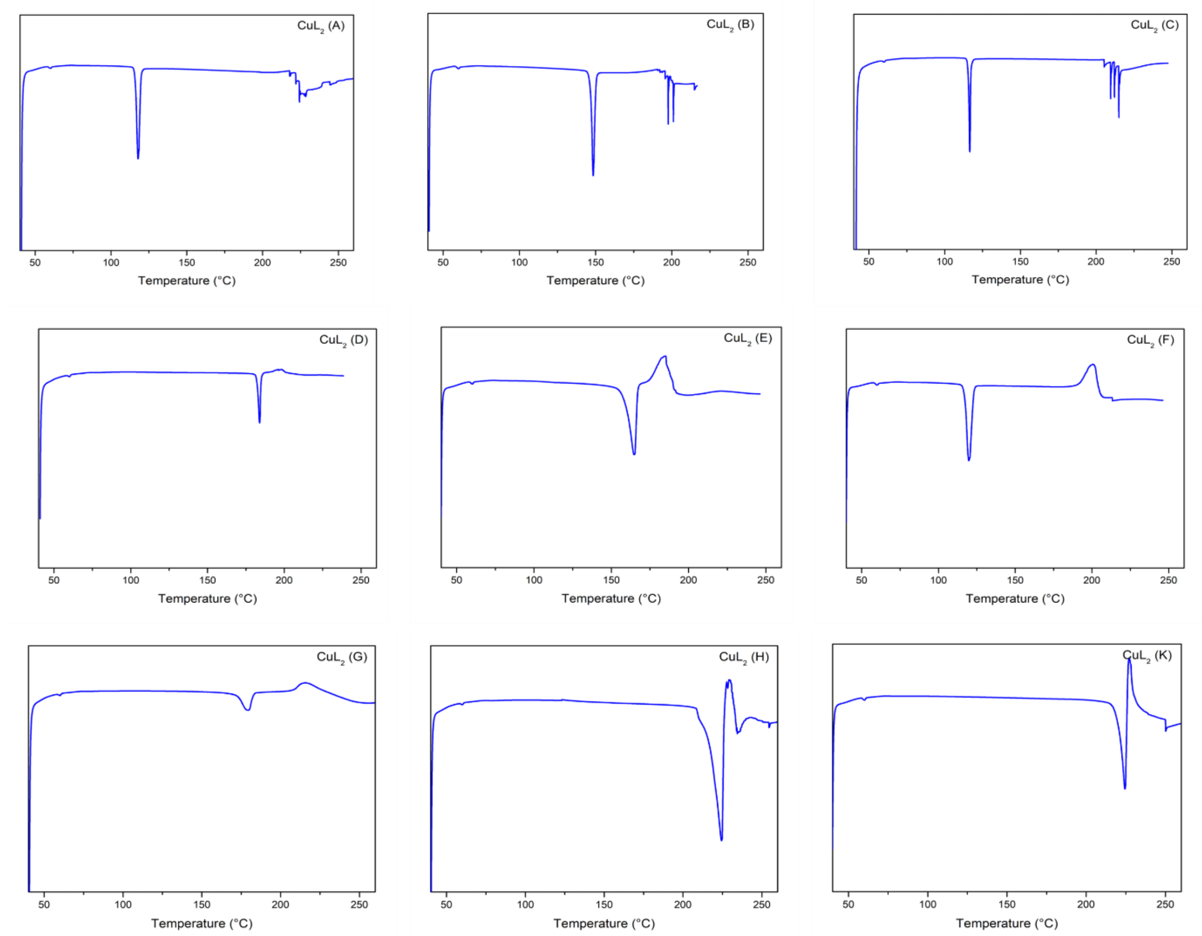

Figure 2 DSC data of copper (II) complexes (A - K). Endothermic peaks ↓ Exothermic peaks ↑.

Isothermal data of the selected precursors (A & B)

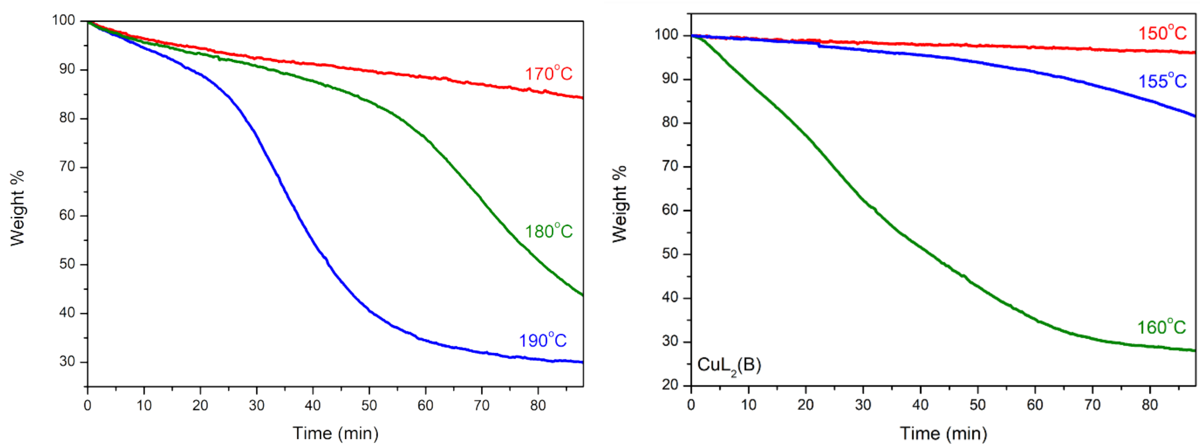

Figure 3 Isothermal TGA of CuL_2(A) Left and CuL_2(B) right.

Table 2 Summary of Isothermal TGA results showing weight loss percentage at set time intervals for both precursors.

Compound	Temperature (°C)	Weight loss %	Period (min)
CuL_2(A)	170	15.70	90
	180	10.22	45
	190	4.19	20
CuL_2(B)	150	4.96	90
	155	4.65	45
	160	8.89	20

Knudsen equation (equation 1) and the Clausius–Clapeyron equation (equation 2)

$$P = \frac{\left(\frac{2\pi RT}{M}\right)^{\frac{1}{2}}\left(\frac{dm}{dt}\right)}{A} \qquad \text{(eqn 1)}$$

Where P = vapour pressure of condensed phase, R = universal gas constant, T = temperature, M = molar mass of sample, A = area and dm/dt = rate of mass loss with respect to time.

$$\log_{10} P = A - \left(\frac{B}{T}\right) \qquad \text{(eqn 2)}$$

Where P = pressure, T = temperature and A and B are constants.

Proof of Principle materials deposition

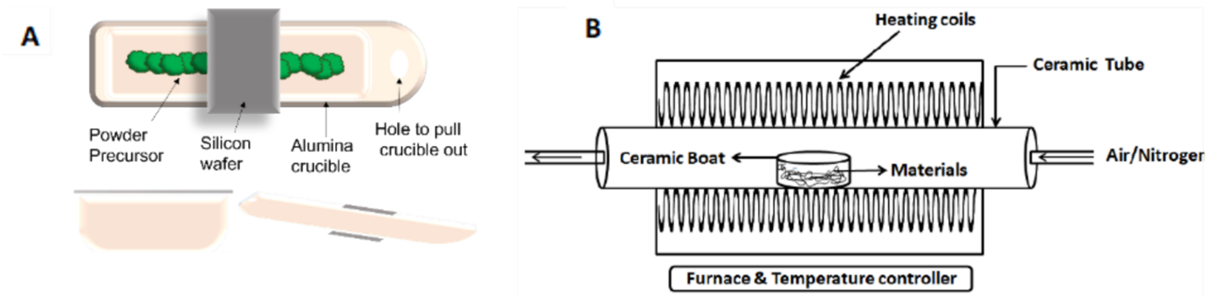

Figure 4 A: Illustration of alumina crucible with wafer placed on top. Figure 4 B: Schematic of tube furnace with crucible.

Schematic of the experimental set up during the CVD growth.

Table 3 Scherrer analysis of crystallite size from precursor (A)

Precursor	K	λ (A)	Peak position 2θ (degrees)	Peak position 2θ (radians)	Cos θ (degrees)	FWHM β (degrees)	FWHM β (radians)	K x λ	D (nm)	Average D (nm)
A	0.94	1.54E-10								
			33.52	0.585034365	0.957521046	0.11686	2.039592E-03		7.41526E-08	74
			48.28	0.842644963	0.912548886	0.09374	1.636072E-03	1.448164E-10	9.69972E-08	97
			55.12	0.962025484	0.886526805	0.06903	1.204801E-03		1.35585E-07	135
			56.84	0.992045147	0.879482495	0.08707	1.519658E-03		1.08354E-07	108
			61.72	1.077217214	0.858423216	0.10767	1.879196E-03		8.97727E-08	89
			62.2	1.085594795	0.856267085	0.08042	1.403594E-03		1.20494E-07	120
				0	1					
				0	1					
									Average A	103.8333333

Table 4 Scherrer analysis of crystallite size from precursor (B)

Precursor	K	λ (A)	Peak position 2θ (degrees)	Peak position 2θ (radians)	Cos θ (degrees)	FWHM β (degrees)	FWHM β (radians)	K x λ	D (nm)	Average D (nm)
B	0.94	1.54E-10								
			33.54	0.585383431	0.957470703	0.11462	2.000496E-03		7.56057E-08	76
			48.3	0.842994029	0.912477494	0.11682	2.038894E-03	1.448164E-10	7.78397E-08	78
			55.2	0.963421747	0.886203579	0.13222	2.307674E-03		7.08125E-08	71
			56.84	0.992045147	0.879482495	0.06996	1.221032E-03		1.34854E-07	134
			61.7	1.076868148	0.858512728		0.000000E+00			
			62.2	1.085594795	0.856267085	0.08314	1.451067E-03		1.16552E-07	116
									Average A	95

Table 5 d-spacing calculations for precursor (A) deposits

Peak position 2θ (degrees)	θ (degrees)	Sin2O	2SinO	λ (A)	d-spacing
33.52	1.68E+01	2.89E-01	5.78E-01	1.54E-10	2.67E-10
48.28	2.41E+01	0.41	8.20E-01		1.88E-10
55.12	2.76E+01	0.46	9.20E-01		1.67E-10
56.84	2.84E+01	0.48	9.60E-01		1.60E-10
61.72	3.09E+01	0.51	1.02E+00		1.51E-10
62.2	3.11E+01	0.52	1.04E+00		1.48E-10

Table 6 d-spacing calculations for precursor (B) deposits

Peak position 2θ (degrees)	θ (degrees)	Sin2O	2SinO	λ (A)	d-spacing
33.54	1.68E+01	2.89E-01	5.78E-01	1.54E-10	2.67E-10
48.3	2.42E+01	0.41	8.20E-01		1.88E-10
55.2	2.76E+01	0.46	9.20E-01		1.67E-10
56.84	2.84E+01	0.48	9.60E-01		1.60E-10
61.7	3.09E+01	0.51	1.02E+00		1.51E-10
62.2	3.11E+01	0.52	1.04E+00		1.48E-10

Table 7 TGA residues actual compared to the theoretical of the deposits and the reference deposits.

Compound	Mw	CuS	Cu	Cu1.8S	Cu1.74S	Cu1.5S	Actual %residue	Theoretical %residue Cu1.74S	Theoretical %residue Cu1.5S	Theoretical %residue Cu1.8S	Theoretical %residue CuS
A	606.43	95.61	63.55	146.46	142.68	127.43	9.1	13.07103321	11.67396805	13.41732214	15.7660406
B	550.32						15.04	14.40374085	12.86423253	14.78533702	17.37352813
C	494.22						17.05	16.03874118	14.32447988	16.46365316	19.34563555
D	590.3						18.44	13.42820035	11.99296027	13.78395166	16.19684906
E	558.22						15.82	14.19989729	12.68217628	14.57609306	17.12765576
F	534.2						16.08	14.83838762	13.25242315	15.23149881	17.89779109
G	642.38						12.66	12.33952904	11.02064891	12.66643835	14.88371369
H	618.36						10.69	12.81885417	11.44874255	13.15846217	15.46186687
K	562.25						14.56	14.09811768	12.59127513	14.47161701	17.00489106

Experimental Information

Compound	TGA mass loading (mg)
A	3.40469
B	7.54240
C	5.72002
D	7.63450
E	4.15861
F	2.75217
G	3.70189
H	2.44313
K	5.74537

Mass loadings of the individual compounds used for their respective TGA analysis.

Compound	Temperature (^{o}C)	Mass loading (mg)
A	170	4.266424
A	180	6.084337
A	190	6.694446
B	150	5.488506
B	155	8.219444
B	160	10.23987

Mass loading for precursor (A & B) at different isothermal temperatures.

Element	Wt %	Δ (std. dev.)	Error Range (3 × Δ)	Reported Value (Wt % ± error)
Si	84.5	0.4	±1.2	**84.5 ± 1.2**
C	8.7	0.4	±1.2	**8.7 ± 1.2**
Cu	3.1	0.1	±0.3	**3.1 ± 0.3**
O	2.8	0.1	±0.3	**2.8 ± 0.3**
S	0.9	0.0	±0.0	**0.9 ± 0.0**

Standard deviation error range of the atomic percentage of each element based on the line EDX from precursor (A) deposit. Cu:S ratio = 1.74 ± 0.17.

Element	Wt %	Δ (std. dev.)	Error Range (3 × Δ)	Reported Value (Wt % ± error)
Si	51.0	0.4	±1.2	51.0 ± 1.2
Cu	22.9	0.2	±0.6	22.9 ± 0.6
C	12.1	0.5	±1.5	12.1 ± 1.5
S	7.8	0.1	±0.3	7.8 ± 0.3
O	6.2	0.2	±0.6	6.2 ± 0.6

Standard deviation error range of the atomic percentage of each element based on the line EDX from precursor (B) deposit. Cu:S ratio = 1.48 ± 0.07.